# Seasonal patterns of water storage as signatures of the climatological equilibrium between resource and demand for the Upper Durance water system

**B. François[1,2], B. Hingray[1,2], F. Hendrickx[3] and J.D. Creutin[1,2]**

[1]CNRS, LTHE – UMR5564, 38041 Grenoble, France

[2]University Grenoble Alpes, LTHE – UMR5564, 38041 Grenoble, France

[3]EDF, R&D, LNHE, 78400 Chatou, France

Correspondence to: B. François *(baptiste.francois@ujf-grenoble.fr)*

**Abstract**

Water is stored in accumulation reservoirs to adapt in time the availability of the resource to various demands like hydropower production, irrigation or ecological constraints. Deterministic dynamic programming retrospectively identifies the reservoir operations that optimize the resource use during a given time period. One of its by-products is the estimation of the marginal storage water value (SWV), defined by the marginal value of the future goods and benefits obtained from an additional unit of storage water volume. The knowledge of the SWV allows determining a posteriori the storage requirement scheme that would have led to the best equilibrium between the resource and the demand. The SWV depends on the water level in the reservoir and shows seasonal as well as inter-annual variations. This study uses the inter-annual average of both the storage requirement scheme and the SWV cycle as signatures of the best temporal equilibrium that is achievable in a given resource/demand context (the climatological equilibrium). For a simplified water resource system in a French mountainous region, we characterizes how and why these signatures change should the climate and/or the demand change, namely changes in mean regional temperature (increase) and/or precipitation (decrease) as well as changes in the water demand for energy production and/or minimum reservoir level maintenance.

In the studied case, the temporal equilibrium between water resource and demand either improves or degrades depending on the considered future scenario. In all scenarios, the seasonality of SWV changes when for example earlier water storage is required to efficiently satisfy increasing summer water demand. Understanding how SWV signatures change helps finally to understand changes in the storage requirement scheme.

**Keywords**: Climate change, Water Resource, Water Demand, Equilibrium, Storage Requirement Scheme, Value of storage water

## 1. Introduction

Mountain catchments yield most of the European hydroelectric production (Eurelectric gives ca. 140 TWh for Scandinavia and the Alps and speaks about the “blue battery” of Europe). At high elevation (and/or latitude), spatial and temporal variations of the snowpack make the hydrological regime of rivers highly seasonal with low and high flows in the snow-accumulation and snowmelt seasons respectively. On the other hand, the electricity demand is also highly seasonal, with consumption peaks that mainly occur during the winter (e.g. Schaefli et al., 2007). The temporal deviations between the resource and the demand can be balanced with storage and release operations, transferring the resource in excess at a given time to times where it is insufficient. Most accumulation water reservoirs in Europe were designed and are managed to phase these two seasonal signals. Many of these reservoirs are not only dedicated to hydroelectricity production but are assigned multiple other management objectives related for instance to low flow maintenance, irrigation and drinking water supply (Loucks et al., 2005). In multipurpose configurations, the time profile of the day-to-day storage levels resulting from storage and release operations aims at the best possible socio-economic equilibrium between water inflows and water demands. This optimal storage requirement scheme (for conciseness also denoted as storage scheme) is thus a signature of the best temporal equilibrium between the natural resource and the demand under a given climate that we call climatological equilibrium.

Significant regional changes are expected worldwide for the next decades as a result of climate change. This will be especially the case for the hydrological regime of mountain rivers. Warmer temperatures will reduce the snow/rainfall ratio and shorten the snow accumulation period. The spring snowmelt will be reduced and shifted earlier in the year by two weeks to one month (Schneider et al., 2013; Lafaysse et al., 2014). Warmer temperatures are also expected to increase the demand for irrigation water (Rosenberg et al., 2003; Rosenzweig et al., 2004) and to modify the seasonal pattern of electricity demand, with lower consumption for heating during the winter and greater needs for cooling during the summer (Alcamo et al., 2007; Hekkenberg et al., 2009). As a result, climate change is expected to modify the seasonal disequilibrium between water availability and demand (Raje and Mujumdar, 2010).

A number of recent studies explored the potential impact of climate change on water systems (e.g. Gaudard et al. 2013). They are mostly based on the simulation of the system management over future periods and the statistical analysis of simulation outputs in terms of system performance. The system simulation is classically based on day to day system operation scenarios obtained with either simple management models based on rule curves or balance equations (Veijalainen et al., 2010; Ashofteh et al., 2013) or more sophisticated models mimicking a real operational context (e.g. Minville et al., 2009; Raje and Mujumdar, 2010; Vicuña et al., 2010). System performance is estimated using synthetic criteria such as the mean benefit from hydropower/agricultural production or the so-called RRV criteria (RRV stands for Reliability, Resilience, and Vulnerability), a statistics of system failures such as day to day deviations between the effective supply and the demand (Hashimoto et al., 1982; Moy et al., 1986). Performance criteria are not easy to interpret alone as i) they may combine resource/demand modifications and management adaptability issues and ii) they summarize behind a single value quite complicated time patterns. Namely, they do not inform if the tested management rules have to be modified and if any better rules exist. They do not describe the possible modification of the temporal resource/demand equilibrium over the considered period even though understanding the time patterns behind this modification is likely to highlight the reasons for modifications of the system performance.

In the present work, we use the mean inter-annual pattern of the storage requirement as a first signature of the evolution of the climatological resource/demand equilibrium. We also consider the marginal value of/for storage water (SWV) representing the future benefit that would be obtained at any given time from an additional unit of water volume stored in the reservoir. We estimate it as a by-product of deterministic dynamic programming (Masse, 1946; Bellman, 1957). The variations of SWV with time for different levels in the reservoir drive the day-to-day storage scheme required to maximize a chosen benefit function coupling water inflows, demand and constraints. They provide a quite detailed description of the role played by the reservoir in redistributing the water throughout the year and from one year to another given the constraints. We propose the mean inter-annual pattern of SWV as an alternative signature of the resource/demand disequilibrium.

The present study looks at how these signatures are modified by changes in climate or demand. We compute both signatures under the present climate and a set of future climate scenarios, for a simplified water resource system with a single storage reservoir. This system is inspired from a real catchment located in the Southern French Alps. We analyze the signature sensitivity to a mean regional temperature increase and/or precipitation decrease. We also explore the influence of the nature of water demand on both signatures (energy production and/or water level maintenance).

The paper is organized as follows. Section 2 briefly describes how the SWV are estimated and how they are used for the determination of the storage scheme. Section 3 presents the simplified water resource system, the data and the simulation models considered in the application to the Upper Durance River (France). It also describes the future climate scenarios considered in this work. The storage scheme of this system is presented and discussed in Section 4. The inter-annual pattern of SWV through the calendar year for the present and future climates are presented and discussed in Sections 5 and 6, when they are interpreted as signatures of the climate change. Section 7 presents the conclusions.

## 2. Storage water values and storage requirement scheme

As mentioned in introduction, the optimal storage requirement scheme is the day-to-day storage level required over the analysis period [$t_0$, $t_N$] to reach the best possible equilibrium between water resource and demand, given operational constraints. This scheme maximizes over the period the sum of the benefits at each time step $t_i$ of the analysis period, plus the benefit expected from the water remaining in the reservoir at the end of the period. The benefit function for any time step, further referred to as the "current" benefit function, can be expressed as a weighted sum of i) the benefits for the current production of different services and goods and/or ii) the costs resulting from the non-satisfaction of constraints related to downstream water demand or to other objectives assigned to the water system. This function thus reads:

$$g(u_{t_i}, s_{t_i}, t_i) = \sum_j c_j \, . \, g_j(u_{t_i}, s_{t_i}, t_i) \qquad 1$$

where $g_j$ is a function representing the monetary benefits and costs associated to the different services by operation $u_{t_i}$ at the storage level $s_{t_i}$ during [$t_i$, $t_{i+1}$] and $c_j$ is a weighting constant defined according to the priority level assigned to use *j*.

For each time step $t_i$, an immediate use of water reduces the availability of stored water for future use. The current benefits must therefore be balanced against losses in future benefits. Identifying the optimal storage variation at the current time step requires knowing the marginal value of conserving water (SWV) in the reservoir from the current time step to the next.

As shown in Appendix A and discussed below, the SWV is time and storage level dependent. It can be obtained a posteriori as a by-product of deterministic dynamic programming, an optimization method developed by Masse (1946) and Bellman (1957) for multistage dynamic decision processes. In our case, they are estimated for the whole analysis period at a daily time step for 51 storage levels uniformly distributed between the minimum and maximum storage bounds $s_{min}$ and $s_{max}$. At any given day, these SWV can be used in a second optimization stage to identify the optimal storage variation given the current water storage in the reservoir. For a given storage level at the beginning of the analysis period, the forward day-to-day optimization process therefore gives the optimal storage requirement scheme for the whole analysis period.

In the following, the SWV is expressed in value units per cubic meter denoted as SWV $m^{-3}$.

# 3. Case study and data

## 3.1. Catchment characteristics and experimental setup

The Upper Durance River (UDR) basin at Serre-Ponçon is a meso-scale basin (3580 $km^2$) located in the southern French Alps. Its outlet is the Serre-Ponçon reservoir, a storage reservoir that is part of a large hydroelectric system operated by Electricité de France (EDF). It plays a key role in the energy supply of the Provence region, which extends from the Alps to the Mediterranean shore, and which is limited in term of energy imports. Its objectives and constraints are also related to recreational activities on the lake, drinking and irrigation water supply and to the preservation of downstream ecological integrity. Contrary to most French mountain basins of this size, UDR discharges are almost natural. The local climate is much drier than in the northern French Alps (Durand et al., 2009) due to the Mediterranean influence and to the protection from oceanic disturbances provided by the high Ecrins Mountains. With elevations ranging from 700 to 4100 m asl, the catchment presents highly seasonal flows due to snow accumulation and melt. Winter low flows can last three months or more. Long low flow sequences are also frequently observed in late summer and fall. They can last several weeks after the end of the snow-covered period for years with negligible precipitation during these seasons. Major floods are often observed in fall with intense liquid precipitation events (Lafaysse et al., 2011).

In this study, we consider a simplified water resource system inspired by the UDR System with two basic uses: hydroelectric production (HEP) and/or maintenance of a minimum water level in the reservoir lake during the summer season for recreational activities such as water sports or fishing (Reservoir Level Maintenance denoted as RLM). As we will see below, we chose HEP and RLM because these two objectives present important differences in terms of adequacy with the water resource availability and are important for the real system of Serre-Ponçon.

The current benefit function used in equation [1] for the determination of SWV is the sum of the possible benefits from HEP as defined by equation [2] and benefits from RLM during a summer season as defined by equation [3]:

$$g_{HEP}\left(u_{t_i}, s_{t_i}, t\right) = HEPI_{t_i}.u_{t_i}.r(s_{t_i}) \qquad 2$$

where $u_{t_i}$ in $m^3\ s^{-1}$ is the discharge released from the reservoir for HEP, HEPI being the daily interest of HEP in value units $kWh^{-1}$ (see section 3.4) and *r* being the hydropower production coefficient in $kWh\ m^{-3}\ s$ that depends on the water head in the reservoir.

$$\begin{cases} g_{LLM}\left(s_{t_i}, t_i\right) = K\left[1 - b\left\{\max\left(s^* - s_{t_i}, 0\right)\right\}^2\right] \ if\ t_i \in summer\ season \\ g_{LLM}\left(s_{t_i}, t_i\right) = 0\ \ if\ not \end{cases} \qquad 3$$

In equation [3], *K* is the maximal value of daily benefit (value units) that can be obtained during the summer period. It is achieved as soon as the storage is greater than a threshold s*= 85 % of the storage capacity, the volume below which recreational activities are expected to be reduced. The corresponding decrease in RLM benefit is assumed to be a quadratic function of the difference between the actual water storage and $s*$. In equation [1], the values of the weighting parameters $c_j$, are referred to as $c_{HEP}$ and $c_{RLM}$ for the HEP and RLM objectives respectively and set either to 1 when the objective is considered or to 0 when it is not.

In the water balance of the reservoir, the only input and output discharges are respectively the inflow from the upstream UDR basin and the optimized water release. Direct precipitations to the reservoir and evaporation from the reservoir are neglected. Their inter-annual mean are actually of the same order, and the net balance between both terms is less than 1 % of the mean river discharge into the reservoir (Vachala, 2008).

In France like in many countries where hydropower is not dominant, hydroelectric production is used to replace more expensive power generation facilities and the objective is to minimize the expected sum of other energy production costs for the national network as a whole. In this study, we consider a simplified daily interest of HEP estimated from a local daily temperature index (see section 3.3) and the benefits are optimized for the system independently from other energy production cost considerations. On the other hand, summer RLM is currently a priority objective: an empirical guideline curve is used for reservoir operations (applied mostly in the spring season) and HEP optimization roughly applies to the water inflows that are not needed to satisfy the RLM objective.

The expected increase of future energy costs will increase the interest of HEP and, as a consequence, benefits from recreational activities will be balanced on the midterm with respect to benefits from HEP (or with respect to the reduction of other production costs allowed by HEP). In this study, a benefit function (equation [3]) is therefore used for RLM instead of a rule curve. This provides a rough estimate of the marginal value of storage water to satisfy the RLM objective. Recreational benefits are expressed as a function of water storage in the reservoir, similarly to Ward et al., (1996). However, our formulation does not include information about tourist affluence due to the lack of appropriate data in the region. The value of $K$ in equation [3] is chosen so that, in the case of a single-objective configuration, the maximum benefits that could be respectively obtained from either RLM or HEP are of the same order of magnitude. This allows analyzing a double-objective configuration with objectives of equivalent economic value, a situation that could occur in the future.

Inflows to the reservoir are modeled with CEQUEAU (Morin et al., 1975), a semi-distributed hydrological model already applied by EDF for previous climate change impact studies on different mesoscale French basins. Snow accumulation and melt, effective rainfall, infiltration and evapotranspiration fluxes are estimated for each of the 99 hydrological units of the basin from daily series of mean areal precipitation and surface air temperature. The discharges produced by all hydrological units are routed through the river network to produce the total water inflow into the reservoir. The CEQUEAU model of UDR has been calibrated and validated with a split sample test procedure (Bourqui et al., 2011). The Nash-Sutcliffe efficiency criterion (Nash and Sutcliffe, 1970) is 0.86 for the 1981-2005 calibration period and 0.83 for the 1959-1981 validation period.

### 3.2. Climate scenarios

The observed precipitation and temperature data for the 1970-1999 control period are obtained from the daily meteorological reanalyses developed by Gottardi et al. (2012) for French mountainous regions. The reference discharges to the reservoir for the control period are those obtained from CEQUEAU simulations.

The local-scale time series of temperature and precipitation for the future climate period 2070-2099 are obtained by perturbing the observed time series of the control period in a similar way to Horton et al., (2006). Six synthetic regional climate change scenarios are defined as an absolute change of the mean annual temperature and as a relative change of the mean annual precipitation. The magnitude of these changes is derived from a suite of climate modeling experiments conducted in the EU PRUDENCE project (Christensen, 2004) for SRES scenario A2 (Nakicenovic et al., 2001). It roughly corresponds to the $50^{th}$ and $90^{th}$ percentiles of changes estimated by the climate model experiments, representing respectively a 10 % and 20 % decrease in precipitation and a 3°C and 5°C increase in temperature.

Future hydrological regimes obtained from CEQUEAU simulations for these scenarios are presented in Figure 1. A temperature increase leads to reduced snow accumulation in winter and an earlier melting season. This in turn induces a higher winter low flow and a lower snowmelt flood peak (Figure 1 left). The snowmelt flood peak shifts by one month for the warmest scenario (+5°C). Besides this change in flow seasonality, an increase in temperature also leads to a slight reduction of the mean annual inflow to the reservoir due to increased evapotranspiration losses in summer (up to 22 % for the +5°C scenario). Without temperature change, precipitation change scenarios modify the magnitude of the hydrological cycle (Figure 1, middle). The mean inter-annual daily discharges decrease with the mean inter-annual precipitation, except for the winter period during which flows are sustained by deep underground storage. The large decrease of the snowmelt flood peak is the result of a smaller snowpack extent and thickness, induced by less winter to spring solid precipitation.

Scenarios with both precipitation and temperature changes lead to a modification of the hydrological regime that roughly combines the modifications previously discussed for temperature change (mainly modification in seasonality) or precipitation change alone (mainly modification in mean discharge).

### 3.3. Economic interest of hydroelectric production

As explained in section 3.1, a detailed representation of electricity prices is difficult to simulate because of the complex interaction with other energy production means and the high variability of the energy market. However, electricity prices in France tend to be higher for periods of high electricity consumption. Moreover, electricity consumption is higher during the cold season and highly correlated with the daily time variations of regional temperatures below an approximate heating threshold $T_{heat}$= 15°C that governs heating demand. As a result, a convenient formulation for the daily interest of HEP (HEPI) can be based on daily regional temperatures like in a previous climate change impact study by EDF (Paiva et al. 2010). The electricity consumption is assumed to linearly decrease with the temperature up to a given threshold and to remain constant above this threshold.

In a future climate with higher summer temperatures, an additional demand for hydroelectric production is expected for cooling purposes. The daily HEP interest expected in the future during the hot season is assumed to linearly depend on regional temperatures above a cooling threshold $T_{cool}$ = 25°C (like in Buzoianu et al. 2005). In the following, the daily HEPI is therefore defined as a piece-wise linear function of daily temperature:

$$\begin{cases} HEPI_{t_i} = HEPI_0 + HEPI_h.\left(T_{heat} - T_{t_i}\right) & if\ T_{t_i} < T_{heat} \\ HEPI_{t_i} = HEPI_0 & if\ T_{heat} < T_{t_i} < T_{cool} \\ HEPI_{t_i} = HEPI_0 + HEPI_c.\left(T_{t_i} - T_{cool}\right) & if\ T_{t_i} > T_{cool} \end{cases} \quad 4$$

where $HEPI_0$ is the HEPI when temperatures are in-between cooling and heating temperature thresholds, $HEPI_h$ and $HEPI_c$ are the additional HEPI rates for each the heating and the cooling seasons respectively. The HEPI is expressed in value units per kWh denoted V hereafter. $HEPI_0$ and $HEPI_h$ are set to unity (=1 V °C$^{-1}$) in accordance to Paiva et al. (2010). A higher value was set for $HEPI_c$ ($HEPI_c$ = 2.5 V °C$^{-1}$).

Time series of daily HEPI were obtained for each scenario of daily temperatures. The corresponding mean inter-annual values of daily HEPI are presented in Figure 2 as typical seasonal HEPI patterns.

## 4. Storage signature

In order to briefly illustrate the kind of climate signature proposed in this work, we start the analysis of our results looking at the storage scheme obtained for the period 1970-1999 when both HEP and RLM objectives are taken into account (this configuration is denoted HEP+RLM in the following). The reservoir inflows and HEPI scenarios are produced as described in Section 3. Their optimal temporal balance is computed through dynamic programming as explained in Section 2. The constrained summer season for RLM runs from June 15$^{th}$ to August 31$^{st}$ and the minimum assigned storage level is $s^*$= 85 % of $s_{max}$ during this period, $s^*$= 0 outside this period. As shown Figure 3, the storage scheme presents a significant seasonality. The storage level continuously decreases during winter months, when HEPI is high and inflows are low. It then increases during spring time with high spring snowmelt inflows and lower HEPI values. The inter-annual variability of the storage scheme is moderate, and much lower than the intra-annual variability that covers the full capacity range from 10 % to 100 % (see dispersion between gray curves around the mean inter-annual pattern in Figure 3). The lowest inter-annual variability of the scheme is obtained for the first days of November. Each year, the reservoir is roughly full at this period. The highest inter-annual variability of the scheme is during spring period when storage levels vary from 10 % to 60 % of the reservoir capacity. All storage curves converge next rapidly to a high storage level as required by the summer touristic level objective. Despite of this, the summer level objective (i.e. 85 % of $s_{max}$) is never reached on time (i.e. the 15$^{th}$ June) but roughly one month later.

In the following, because the temporal variations of the storage scheme are mainly seasonal, we use its mean inter-annual pattern a first signature of the disequilibrium between water resources and demand for the studied climatic and economical forcing. We call it for short, the storage signature.

## 5. Storage water value signature

The storage signature derives from temporal patterns of SWV that we discuss now for various climate scenarios and various combinations of objectives. For a more comprehensive analysis, we consider in a preliminary step two objectives separately (HEP or RLM) and subsequently a double-objective configuration (HEP+RLM).

### 5.1 Hydroelectric production

The optimization of the HEP objective alone corresponds to $C_{HEP}$=1 and $C_{RLM}$=0 in equation [1]. Note first that the efficiency of the hydroelectric production system is an increasing function of water head in the reservoir. If HEPI were constant throughout the year, the storage scheme would be to maintain the water level at its highest possible value, which may be a bit lower than the full reservoir level to avoid future spillage (see for example Turgeon, 2007). Except before large inflow periods such as the snowmelt season, this scheme would correspond to high SWV for most reservoir levels, especially the lowest ones. In the studied configuration, the storage scheme is of course modulated by the high seasonality of HEPI, SWV being higher during the periods before highest HEPI.

Figure 4 illustrates the variation of the HEPI and the water inflows to the reservoir with time over a four-year period ($1^{st}$ January 1977 to $1^{st}$ January 1981). It also presents the corresponding variations of the SWV with time for different reservoir levels (corresponding to 10 %, 50 % and 90 % of storage capacity) and the resulting optimal storage requirement scheme.

At any time, SWV is lower at high storage levels (Figure 4-top) when more water is actually available for future use and also when the risk for future water spillage is high. In other words, surplus storage water would need to be turbined during periods with lower HEPI or worse to be spilled if necessary. At high storage levels (e.g. 90 % storage level), SWV is therefore low except in the case of an imminent period with very high HEPI that justifies storing more water (e.g. during winter periods). At low storage levels (e.g. 10 % storage level), SWV is conversely high to very high (up to 10 value units), except during periods with high future inflows (e.g. during spring periods). At all storage levels high SWV prompts water storage for future use.

Broadly speaking, periods of high HEPI alternate with periods of high inflow discharges (Figure 4-bottom), and consequently SWV presents high seasonal variations for all reservoir levels (Figure 4-top). During the late winter and early spring transition period, the requirement for more storage water decreases as a result of the concomitant decrease of HEPI and the rapid increase of snowmelt inflow. The following increase of SWV is quite abrupt and begins as soon as spillage is no longer required for the known future inflows. For the year 1979, this increase can be seen for example in June for a storage level of 50 % and in September for a storage level of 90 % due to a large flood event that occurred in fall of this year. The storage scheme increases the water storage for the following winter (Figure 4-middle).

For any given storage level, SWV varies with time reflecting the role of the reservoir in adjusting the adequacy between the future HEPI and the future availability of water from upstream catchments. Future resource abundance (respectively scarcity) decreases (respectively increases) the value of more storage water like for example in May 1977 (respectively September 1977).

In addition to a marked seasonality, SWV shows year-to-year variations related to the future ratio of HEPI and the inflow. SWV is for instance higher in 1980 than in the previous three years. This inter-annual variability directly translates to the storage requirement scheme with a spring storage higher than 30 % of the capacity for 1980 whereas it roughly equals to zero for previous years.

The variation of SWV with time like the storage requirement thus reflects in a sophisticated way the temporal patterns of the climate variables governing the water demand and inflows. In the following we will use the mean inter-annual patterns of SWV for different reservoir levels as a second signature of the disequilibrium between water resource and demand under climatic and economic conditions. The SWV signature obtained for the studied UDR system is presented Figure 5 for three storage levels (10 %, 50 % and 90 % of storage capacity). In addition to the mean inter-annual value, Figure 5 also shows the $5^{th}$ or

95th percentiles of the SWV calendar values. For the sake of conciseness, the expression "SWV signature" will subsequently be used for this type of graphs.

**5.2 Summer reservoir level maintenance**

We now consider a system for which the only objective would be to maintain a minimum water level in the reservoir during the summer months as explained in Section 3 (i.e. $C_{HEP}$=0 and $C_{RLM}$=1 in equation [1]). Penalty costs are incurred in the event of failure to maintain the required level. The SWV corresponds to the additional reduction of penalty costs that would be achieved by storing one more cubic meter of water at the current date. The SWV signature is quite different from the one obtained for the HEP objective alone although it presents also a marked seasonality (see Figure 6 compared to Figure 5).

The possibility to achieve the objective depends on the current storage level and on the volume of inflow that will enter the reservoir from the current date to the beginning of the next constrained period. At a given date, the higher the current storage level, the easier it is to achieve the objective.

For a given storage level, the longer the duration until the next constrained period, the larger the total future inflows to the reservoir and the easier it is to reach the objective. SWV therefore slowly increases over the year to reach a maximum in early summer. According to Figure 6 the SWV maximum is nearly one month before the beginning of the constrained period for the most adverse situations (95th percentile envelope curve – corresponding to the driest spring years) or as late as mid-July for the most favorable situations (5th percentile envelope curve – corresponding to the wettest spring years). The lowest SWV is zero, indicating that there is no interest to store water as forthcoming inflows will fill the reservoir to the required level on time (Figure 6). This is the case for almost all reservoir levels in September, after the end of the constrained period (an exception is for the driest years if the storage level is low). This applies also from mid-September to mid-April at more than 50 % of the storage capacity when large inflows from the spring snowmelt flood are expected.

In terms of seasonality the periods of high and low SWV are roughly in phase opposition with those obtained previously for the HEP objective.

**5.3. Double-objective configuration**

Figure 7 presents the SWV signature obtained when both HEP and RLM objectives must be fulfilled (i.e. $C_{HEP}$=1 and $C_{RLM}$=1 in equation [1]). The storage signature for this configuration is the one discussed in Section 4 (Figure 3).

For this configuration, SWV is logically higher than those obtained for each single-objective configuration (Figure 5 and Figure 6). It is actually not possible to produce as much HEP and to fulfill the RLM objective as well as in the single-objective configurations. To limit the costs of RLM failures, water allocations previously determined for the single HEP objective configuration must be re-allocated to periods with lower HEPI thanks to higher SWV at all reservoir levels, since high SWV reduces the interest of immediate water use.

The SWV signature for the double-objective configuration is not exactly an additive combination of the two single-objective signatures owing to the non-linearity of the optimization. The most significant difference between the HEP+RLM signature and the sum of the single-objective ones is during the winter season at low reservoir levels. The higher SWV obtained for the double-objective configuration directly translates to the storage scheme. For instance, the minimum storage levels of the storage scheme are all greater than 10 % (see Figure 3) whereas it can reach zero in the single HEP objective configuration (see spring storage level for the year 1977 in Figure 4). Similarly, the storage level in the early fall is always over 80 to 90 % in the double objective configuration, whereas it may be lower than 80% in the single HEP objective configuration (see year 1979 in Figure 4).

In summary, the SWV signature displays patterns of increasing complexity when the variety of assigned objectives increases. The seasonal shapes of the different objectives combine almost linearly and reflect with great detail the respective seasonality of the climate and the various demands.

## 6. Sensitivity of the signatures to climate change

We show now the sensitivity of the storage and SWV signatures to a climate modification resulting from in annual temperature increase, an annual precipitation decrease and finally from both modifications simultaneously. This sensitivity analysis illustrates the interest of the presented results in terms of climate change signatures.

Figure 8 displays the storage signature for the double-objective configuration HEP+RLM. As observed on the figure, the signature is more sensitive to temperature warming than to precipitation decrease. For all scenarios, the average storage levels increases and the magnitude of seasonal storage fluctuation is significantly lower which means that the resource-demand temporal equilibrium improves under the considered future climates. The temporal pattern of the storage signature is also modified: the late summer period for which high levels of storage were required is two months longer for a 3°C warming. For the 5°C warming scenario, a bimodal pattern is obtained and the period with the highest required storage levels is shifted to early summer.

Figure 9 shows the dependence of SWV signatures to temperature for different objectives. For the HEP objective alone (first line Figure 9), a temperature increase modifies the seasonality of the SWV signature but does not significantly change the average value of storage water. The SWV seasonal peak is shifted from autumn to summer for high reservoir levels and disappears at low levels. At all levels the seasonality of SWV is smoothed out; in particular for low and medium reservoir levels (10 and 50 %), SWV becomes practically constant throughout the year. This observation corroborates the better temporal balance between resource and demand under a modified climate. At low and middle storage levels and compared to the control period, the increase of during the spring season is due to far less intense snowmelt floods (Figure 1) and in turn to a large decrease of potential spillage risk. Potential spillage is also reduced because of a better temporal match between inflows and periods of high HEPI: for the control period, the main inflow period (spring) is almost 8 months before the highest HEPI (winter); for the increased-temperature scenarios, the snowmelt flood is up to one month earlier and a second period with high HEPI appears in the summer season only 3 to 4 months later.

At high storage level, the SWV signature modification is different but the reasons for these changes remain the same. The large SWV values during the late spring and summer seasons increase the interest of raising the water head during this period without causing later spillage thanks to the new and greater interest of HEP in summer. The low SWV values in winter result from the lower HEPI demand for this season.

For the RLM objective alone, lower mean inflow and earlier snowmelt increase SWV earlier in the year for reservoir levels lower than the summer objective. The objective is therefore more difficult to meet on time than for the control period. For low reservoir storage levels the positive SWV obtained in September even shows incapacity to meet this single objective.

Finally, the SWV signature obtained for the double HEP+RLM configuration is as for the present climate approximately an additive combination of the two single-objective signatures, as for the present climate. For example, for the 50 % storage level, the large SWV decrease observed in the control climate during the six months from December to May tends to disappear as a consequence of the smaller snowmelt flood and the increased HEP interest during the summer months.

Regarding now a precipitation decrease, Figure 10 displays the SWV signature for the HEP+RLM configuration. As changes in precipitation do not influence the seasonality of the inflow (Figure 1) and the demand, the seasonality of SWV is maintained, whatever the reservoir level. The decrease in precipitation leads to a reduced mean inflow to the reservoir and in turn, to an increased SWV mean value at all storage levels and all seasons (excepted during the summer season for the 90 % storage level where SWV is zero). This means more severe conditions with a concentration of water allocations to HEP in the periods with the highest HEPI.

Finally, the SWV signature resulting from a modification of both precipitation and temperature changes is shown for three storage levels in Figure 11. Seasonality and mean value of SWV are modified. Changes of SWV for this combined change are approximately an additive combination of the partial ones, and directly translate to modifications of the storage scheme described previously. They lead for instance to building the storage earlier in order to better use the earlier spring snowmelt flood. They also lead to reducing the magnitude of storage fluctuations and thus to increase the water head, especially before the period of high HEPI in summer due to cooling needs.

## 7. Conclusion

In this study we formalize the central role of water storage management in balancing seasonal fluctuations of the water resource/demand equilibrium using an elementary optimization technique. The representation of the water system is reduced to a small set of objectives and free of any hypothesis on the real time management constraints and uncertainties. Derived storage water values and reservoir levels exhibit seasonal patterns that we propose to read as signatures of this climatological equilibrium and its potential modification under changing hydro-climatic conditions. We consider such signatures as attractive alternatives to bulk indicators like statistics of system failures in the sense they preserve quite complicated seasonal patterns giving more insight into the socio-technical system behavior.

The presented case study illustrates how the proposed signatures contain, under a synthetic set of graphs, much information on the seasonality of the governing processes and their eventual shifts in time. The studied multi-purpose system taken in the French Alps is reduced to the management of a single reservoir responding a twofold demand for hydroelectricity and reservoir level maintenance during a touristic period in a climate change context. This case study leads to the following considerations.

When considering several management objectives, each individual objective signature sheds light its specific role and the multi-purpose signature is not the mere linear combination of the individual signature, which reveals the potentially non-linear interaction or competition between objectives.

When analyzing signatures one by one, the smoothness of their shape and their amplitude looks to be informative. Both for SWV and storage patterns, a smoother shape shows a better seasonal fit between resource and demand and thus an easier manageability or lower storage fluctuation needs.

When comparing signatures under different climatic conditions, changes in shape reveal changes of the governing processes. For instance, the studied water system seems to be more sensitive to warmer conditions than to dryer ones. Warmer conditions deeply modify the different signatures (SWV and storage) in relation with the behavior of the snow-pack and the electricity demand. Dryer ones provide more homothetic shape modifications, revealing less impact on the management and the storage patterns.

As a last consideration, we can note that the storage signature is more straightforward to interpret both in term of shape (management difficulty) and amplitude (reservoir relevance). Nevertheless, this signature only reflects the satisfaction of the objective and its shape can be weakly informative when this objective is simple like in the case of the RLM alone – the storage signature is then almost flat throughout the year. Interpreting SWV signatures requests a more economical reasoning about the interest of water allocation in time. It expresses in more details the all set of mechanisms behind the satisfaction of the assigned objective. In the case of the RLM objective alone for instance, the SWV will display the rather marked seasonality of the needed management and not only its mere result. In that sense, we suggest that both signatures are useful.

The proposed study shows different limitations opening new working perspectives. They are for instance relative to the complexity of the system used for the demonstration. Real water resource systems deal generally with more objectives and constraints and with a number of interconnected reservoirs. With an optimization algorithm such as dynamic programming, additional constraints and requirements can be integrated quite easily (e.g. irrigation water demand, dam safety management during floods or minimum flow maintenance for ecosystem integrity). In the case of multi-reservoir systems, SWV will be site dependent in addition to be time and storage level dependent (Tilmant et al., 2008, 2009; Wolfgang et al., 2009).

The simulation of future hydrological scenarios was here driven by observed precipitation and temperature time series modified according to synthetic climate change scenarios using a classical perturbation methodology. The temporal variability of future meteorological variables is therefore the same as that of the historical period. In particular, no changes in the sequences of wet and dry periods are considered from seasonal to pluri-annual time scales. Such changes are however expected to be potentially as critical as changes in the means of meteorological driving variables. They at least fully determine changes in the temporal variability of natural inflows into a reservoir, a determinant factor in system performance (McMahon et al., 2006). Changes in precipitation seasonality are for instance expected to modify the seasonality of inflows. A higher variability of annual or pluri-annual inflows into the reservoir is also expected to lead to longer and/or more frequent periods of resource scarcity. The influence of such regional climate modifications will be analyzed with scenarios recently developed for the studied region using different statistical downscaling models from a suite of GCM experiments (Lafaysse et al., 2014).

Note finally that SWV is also frequently estimated for determining an operating strategy for real-time management of a water system. In such a case, the SWV can be obtained using stochastic dynamic programming in a configuration in which future inflows and water demands are unknown (e.g. Wolfgang et al., 2009). As a result of inflow variability and imperfect forecastability, the SWV is expected to increase when compared to the SWV obtained in the configuration of the present work (Draper et al., 2003; François, 2013). SWV signatures obtained for an uncertain future are also potentially very informative with regard to how an operational strategy is organized, what its key features are and how it could change should the climate and/or demand change. When they are conversely obtained for a known sequence of inflow and demand, as in the present work, SWV define the best possible manageability of the system. They are therefore not influenced by possible changes in the forecastability of future inflows and demand and they separate in a sense the socio-climatic and the management components of the equilibrium. To this respect, analyzing changes in this signature is expected to improve our understanding of modifications of the optimal storage requirement scheme for this socio-climatic context as well as modifications of system performance classically reported on the basis of a variety of performance criteria in climate change impact analyses.

## Acknowledgement

This work is part of a PhD thesis carried out within the RIWER2030 research project http://www.lthe.fr/RIWER2030/, funded by the French National Research Agency under the Vulnerability: Environment, Climate and Societies program (Grant number ANR-08-VULN-014-01). The authors thank Ehret Uwe and two anonymous reviewers for their comments and suggestions which helped to improve this manuscript.

## Appendix

In deterministic dynamic programming, the optimal storage variation for each time step $t_i$ of the considered simulation period [$t_0$, $t_N$] is identified in order to maximize the sum, over the simulation period [$t_i$, $t_N$], of the current benefits, i.e. the benefits that would result from an immediate use of water at time step $t_i$, and of the optimal future benefits, i.e. the benefits that would result from optimal storage variations over the future simulation period [$t_{i+1}$, $t_N$]. The optimal future benefit $F_{t_i}(s_{t_i})$ obtainable from a hypothetical reservoir level $s_{t_i}$ at time $t_i$ is often referred to as the Bellman Value for this storage and time configuration (Bellman, 1957). It is obtained from a backward recursive calculation from the future benefits estimated for time $t_{i+1}$:

$$F_{t_i}(s_{t_i}) = \max_{u_{t_i}}\{g(u_{t_i}, s_{t_i}, t_i) + F_{t_{i+1}}(s_{t_{i+1}})\} \qquad \text{A.1.}$$

where the different terms are subject to upper and lower bounds and mass conservation constraints. The state and decision variables are such that:

$$s_{min} \leq s_{t_i} \leq s_{max} \qquad \text{A.2.}$$

and

$$u_{min} \leq u_{t_i} \leq u_{max} \qquad \text{A.3.}$$

where $s_{min}$ and $s_{max}$ are minimum and maximum bounds for water storage volumes in the reservoir and $u_{min}$ and $u_{max}$ the minimum and maximum bounds for release discharges. The mass conservation equation is:

$$s_{t_{i+1}} = s_{t_i} + q_{t_i} - u_{t_i} - o_{t_i} \qquad \text{A.4.}$$

where $q_{t_i}$ is the inflow to the reservoir during the period [$t_i$, $t_{i+1}$], $o_{t_i}$ the losses (evaporation above the reservoir, controlled and uncontrolled withdrawals from the reservoir for irrigation, drinking water and other uses).

A discrete approach can be used to estimate the benefit function $F_t(s)$ when the dimension of the state vector is not too large. An extensive discussion about the dimensionality issue is presented in Yakowitz (1982). The final result is a table that gives the future benefits for different water levels and each time step of the simulation period. For storage levels in-between the a priori selected states, $F_t(s)$ can be obtained *via* interpolation. In our case, $F_t(s)$ is estimated at a daily time step and at 51 storage levels uniformly distributed between the minimum and maximum storage bounds $s_{min}$ and $s_{max}$. A cubic spline interpolation method is used when needed (Foufoula-Georgiou and Kitanidis, 1988).

Values of $F_{t_N}(s)$ are required for $F_t(s)$ at the final time $t_N$ of the simulation period. They can have a critical influence on $F_t(s)$ values. Values of $F_{t_N}(s)$ are sometimes obtained from the mean inter-annual values of SWV estimated for the corresponding calendar day. This estimation however requires a first estimate of $F_t(s)$ for the whole simulation period [$t_0$, $t_N$] and thus also a first guess of the end values $F_{t_N}(s)$ from this calculation. An iterative process is thus necessary that may be quite long to achieve convergence. In the present study, end values are estimated as proposed by Wolfgang et al. (2009). The duration of the simulation period is artificially increased with a fictitious *n*-year initialization period, added at the end of the simulation period. The initialization period is composed from several duplications of the final year so that the storage water values at $t_N$ are no longer influenced by the boundary conditions chosen at the end of the extended planning period. The storage water values at $t_N$ are next used to estimate the corresponding Bellman value $F_{t_N}(s)$ from the reciprocal function of equation A.1.

The derivative of the future benefit function $F_t(s)$ for a given storage level *s* in the reservoir gives the optimal benefit for a future use of one additional unit of water stored at this storage level (equation [1]). It corresponds to the marginal value of storage water for this storage level *s* and time *t.*

$$V_t(s) = \frac{\partial F_t(s)}{\partial s} \qquad \text{A.5.}$$

As shown in equation A.5, the marginal value of storage water *V* is time and storage level dependent. The SWV signatures proposed in Section 5 are derived from this computation.

The above mentioned optimization stage provides the optimal future benefit $F_t(s)$ for all storage levels *s* of the state-time table. This table can be used to derive the storage water values *V* for the same state-time grid. In a discrete approach, the derivatives are calculated with finite differences from neighboring water level states in the table.

The storage water values can be used in a second optimization stage to identify the optimal operation decision for the current time $t_i$, given the water level in the reservoir $s_{t_i}$. This operation maximizes the following equation:

$$\max_{u_{t_i}} \{ g(u_{t_i}, s_{t_i}, t_i) + (s_{t_{i+1}} - s_{t_i}).V_{t_{i+1}}(s_{t_{i+1}}) \} \qquad \text{A.6.}$$

The forward iterative optimization of equation A.6 can therefore give the optimal sequence of storage variations, resulting reservoir water levels, benefits and penalty costs over the whole simulation horizon [$t_0$, $t_N$]. This simulation method is usually referred to as the water value method (e.g. Hveding, 1968). The storage signature proposed in Section 4 is derived from this computation.

## References

Alcamo, J., J. M. Moreno, B. Novaky, M. Binidi, R. Corobov, R. J. . Devoy, C. Giannakopoulos, E. Martin, J. . Olesen, and A. Shvidenko (2007), Europe, in Climate Change 2007: Impacts, Adaptations and Vulnerability. Contribution of Working Group II to the

Fourth Assessment Report of the Intergovernmental Panel on Climate Change, pp. 541–580, Cambridge.

Ashofteh, P. S., O. B. Haddad, and M. A. Mariño (2013), Climate Change Impact on Reservoir Performance Indexes in Agricultural Water Supply, Journal of Irrigation and Drainage Engineering, 139(2), 85–97, doi:10.1061/(ASCE)IR.1943-4774.0000496.

Bellman, R. (1957), Dynamic Programming, Princeton University Press., Defense Technical Information Center, New Jersey, 366pp.

Bourqui, M., T. Mathevet, J. Gailhard, and F. Hendrickx (2011), Hydrological validation of statistical downscaling methods applied to climate model projections, IAHS-AISH publication, 344, 32–38.

Buzoianu, M., A. E. Brockwell, and D. J. Seppi (2005), A Dynamic Supply-Demand Model for Electricity Prices, Carnegie Mellon University,Department of statistics. [online] Available from: http://search.stat.cmu.edu/tr/tr817/tr817.pdf (Accessed 11 October 2012)

Christensen, N. (2004), Prediction of Regional scenarios and Uncertainties for Defining EuropeaN Climate change risks and Effects - Prudence Final Report, PREUDENCE EVK2-CT2001-00132. [online] Available from: http://prudence.dmi.dk (Accessed October 2013)

Draper, A. J., M. W. Jenkins, K. W. Kirby, J. R. Lund, and R. E. Howitt (2003), Economic-engineering optimization for California water management, Journal of water resources planning and management, 129(3), 155–164.

Durand, Y., M. Laternser, G. Giraud, P. Etchevers, B. Lesaffre, and L. Merindol (2009), Reanalysis of 44 Yr of Climate in the French Alps (1958-2002): Methodology, Model Validation, Climatology, and Trends for Air Temperature and Precipitation, J. Appl. Meteorol. Climatol., 48(3), 429–449, doi:10.1175/2008JAMC1808.1.

Foufoula-Georgiou, E., and P. K. Kitanidis (1988), Gradient dynamic programming for stochastic optimal control of multidimensional water resources systems, Water Resour. Res., 24(8), 1345–1359, doi:198810.1029/WR024i008p01345.

François, B. (2013), Gestion optimale d’un réservoir hydraulique multiusages et changement climatique. Modèles, projections et incertitudes, Université de Grenoble,

Grenoble. [online] Available from: http://tel.archives-ouvertes.fr/docs/00/99/70/12/PDF/33716_FRANCOIS_2013_archivage.pdf (Accessed 05 June 2014)

Gaudard, L., M. Gilli, and F. Romerio (2013), Climate Change Impacts on Hydropower Management, Water Resources Management, doi:10.1007/s11269-013-0458-1.

Gottardi, F., C. Obled, J. Gailhard, and E. Paquet (2012), Statistical reanalysis of precipitation fields based on ground network data and weather patterns: Application over French mountains, Journal of Hydrology, 432–433, 154–167, doi:10.1016/j.jhydrol.2012.02.014.

Hashimoto, T., J. R. Stedinger, and D. P. Loucks (1982), Reliability, resiliency, and vulnerability criteria for water resource system performance evaluation, Water Resour. Res., 18(1), 14, doi:10.1029/WR018i001p00014.

Hekkenberg, M., R. M. J. Benders, H. C. Moll, and A. J. M. Schoot Uiterkamp (2009), Indications for a changing electricity demand pattern: The temperature dependence of electricity demand in the Netherlands, Energy Policy, 37(4), 1542–1551, doi:10.1016/j.enpol.2008.12.030.

Horton, P., B. Schaefli, A. Mezghani, B. Hingray, and A. Musy (2006), Assessment of climate-change impacts on alpine discharge regimes with climate model uncertainty, Hydrol. Process., 20(10), 2091–2109, doi:10.1002/hyp.6197.

Hveding, V. (1968), Digital simulation techniques in power system planning, Economics of Planning, 8(1), 118–139, doi:10.1007/BF02481379.

Lafaysse, M., B. Hingray, P. Etchevers, E. Martin, and C. Obled (2011), Influence of spatial discretization, underground water storage and glacier melt on a physically-based hydrological model of the Upper Durance River basin, Journal of Hydrology, 403(1-2), 116–129, doi:10.1016/j.jhydrol.2011.03.046.

Lafaysse, M., B. Hingray, J. Gailhard, A. Mezghani, and L. Terray (2014), Internal variability and model uncertainty components in future hydrometeorological projections: The Alpine Durance basin, Water Resour. Res. DOI: 10.1002/2013WR014897

Loucks, D. P., E. van Beek, J. R. Stedinger, J. P. M. Dijkman, and M. T. Villars (2005), Water Resources Systems Planning and Management: An Introduction to Methods, Models and Applications, Paris : UNESCO. [online] Available from: http://ecommons.library.cornell.edu/handle/1813/2804 (Accessed 23 May 2013)

Marnezy, A. (2008), Les barrages alpins. De l’énergie hydraulique à la neige de culture, Revue de géographie alpine. Journal of Alpine Research, 1(96), 92–102, doi:10.4000/rga.422.

Masse, P. (1946), Les réserves et la régulation de l’avenir dans la vie économique, Actualités scientifiques et industrielles 1008, Hermann, Paris.

McMahon, T., A. Adeloye, and S. Zhou (2006), Understanding performance measures of reservoirs, Journal of Hydrology, 324(1-4), 359–382, doi:10.1016/j.jhydrol.2005.09.030.

Minville, M., F. Brissette, S. Krau, and R. Leconte (2009), Adaptation to Climate Change in the Management of a Canadian Water-Resources System Exploited for Hydropower, Water Resour Manage, 23(14), 2965–2986, doi:10.1007/s11269-009-9418-1.

Morin, G., J. P. Fortin, and R. Charbonneau (1975), Utilisation du modèle hydrophysiographique CEQUEAU pour l’exploitation des réservoirs artificiels, IAHS Publication n, 115, 176–184.

Moy, W.-S., J. L. Cohon, and C. S. ReVelle (1986), A Programming Model for Analysis of the Reliability, Resilience, and Vulnerability of a Water Supply Reservoir, Water Resour. Res., 22(4), PP. 489–498, doi:198610.1029/WR022i004p00489.

Nakicenovic, N., Alcamo, J., Davis, G., de Vries, B., Fenhann, J. Gaffin, S., Gregory, K., Grubler, A., Jung, T., Kram, T., La Rovere, E.L., Michaelis, L., Mori, S., Morita, T., Pepper, W., Pitcher, H.M., Price, L., Riahi, K., Roehrl, A., Rogner, H.H, Sankovski, A., Sclesinger, M., Shukla, P., Smith, S.J., Swart, R., van Rooijen, S., Victor, N. et Dadi, Z. (2001), Special Report on Emissions Scenarios : a special report of Working Group III of the Intergovernmental Panel on Climate Change. [online] Available from: http://www.osti.gov/energycitations/servlets/purl/15009867-Kv00FB/native/ (Accessed 20 April 2012)

Nash, J. E., and J. V. Sutcliffe (1970), River flow forecasting through conceptual models part I — A discussion of principles, Journal of Hydrology, 10(3), 282–290, doi:10.1016/0022-1694(70)90255-6.

Paiva, R. C. D., W. Collischonn, E. B. C. Schettini, J.-P. Vidal, F. Hendrickx, and A. Lopez (2010), The Case Studies, in Modelling the Impact of Climate Change on Water Resources, edited by F. Fung, A. Lopez, and M. New, pp. 136–182, John Wiley & Sons, Ltd. [online] Available from: http://onlinelibrary.wiley.com/doi/10.1002/9781444324921.ch6/summary (Accessed 18 May 2012)

Raje, D., and P. P. Mujumdar (2010), Reservoir performance under uncertainty in hydrologic impacts of climate change, Advances in Water Resources, 33(3), 312–326, doi:10.1016/j.advwatres.2009.12.008.

Rosenberg, N. J., R. A. Brown, R. C. Izaurralde, and A. M. Thomson (2003), Integrated assessment of Hadley Centre (HadCM2) climate change projections on agricultural productivity and irrigation water supply in the conterminous United States, Agricultural and Forest Meteorology, 117(1-2), 73–96, doi:10.1016/S0168-1923(03)00025-X.

Rosenzweig, C., K. M. Strzepek, D. C. Major, A. Iglesias, D. N. Yates, A. McCluskey, and D. Hillel (2004), Water resources for agriculture in a changing climate: international case studies, Global Environmental Change, 14(4), 345–360, doi:10.1016/j.gloenvcha.2004.09.003.

Schaefli, B., B. Hingray, and A. Musy (2007), Climate change and hydropower production in the Swiss Alps: quantification of potential impacts and related modelling uncertainties, Hydrology and Earth System Sciences, 11(3), 1191–1205.

Schneider, C., C. L. R. Laizé, M. C. Acreman, and M. Flörke (2013), How will climate change modify river flow regimes in Europe?, Hydrol. Earth Syst. Sci., 17(1), 325–339, doi:10.5194/hess-17-325-2013.

Tilmant, A., D. Pinte, and Q. Goor (2008), Assessing marginal water values in multipurpose multireservoir systems via stochastic programming, Water Resour. Res., 44, W12431, doi:10.1029/2008WR007024.

Tilmant, A., Q. Goor, and D. Pinte (2009), Agricultural-to-hydropower water transfers: sharing water and benefits in hydropower-irrigation systems, Hydrol. Earth Syst. Sci., 13(7), 1091–1101.

Turgeon, A. (2007), Stochastic optimization of multireservoir operation: The optimal reservoir trajectory approach, Water Resour. Res., 43, W05420, doi:10.1029/2005WR004619.

Vachala, S. (2008), Evaporation sur les retenues du Sud de la France (In French), Master Thesis, Université Pierre et Marie Curie, Ecole des Mines de Paris & Ecole Nationale du Génie Rural des Eaux et des Forêts. [online] Available from: http://www.sisyphe.upmc.fr/~m2hh/arch/memoires2008/Vachala.pdf (Accessed 29 October 2013)

Veijalainen, N., T. Dubrovin, M. Marttunen, and B. Vehviläinen (2010), Climate Change Impacts on Water Resources and Lake Regulation in the Vuoksi Watershed in Finland, Water Resources Management, 24(13), 3437–3459, doi:10.1007/s11269-010-9614-z.

Vicuña, S., J. A. Dracup, J. R. Lund, L. L. Dale, and E. P. Maurer (2010), Basin-scale water system operations with uncertain future climate conditions: Methodology and case studies, Water Resour. Res., 46(4), doi:10.1029/2009WR007838.

Ward, F. A., B. A. Roach, and J. E. Henderson (1996), The Economic Value of Water in Recreation: Evidence from the California Drought, Water Resources Research, 32(4), 1075–1081, doi:10.1029/96WR00076.

Wolfgang, O., A. Haugstad, B. Mo, A. Gjelsvik, I. Wangensteen, and G. Doorman (2009), Hydro reservoir handling in Norway before and after deregulation, Energy, 34(10), 1642–1651, doi:10.1016/j.energy.2009.07.025.

Yakowitz, S. (1982), Dynamic programming applications in water resources, Water Resour. Res., 18(4), 673–696, doi:10.1029/WR018i004p00673.

**List of figures**

**Figure 1. Mean inter-annual cycles of daily inflow to the reservoir for control data** (black curve in all graphics, period 1970-1999) **and two future meteorological scenarios** (with prescribed changes of the mean annual temperature ($\Delta T$) and precipitation ($\Delta P$) over the period 2070-2099). Left: Changes in mean annual temperature only. Middle: Changes in mean annual precipitation only. Right: Changes in both annual precipitation and temperature. The control hydrological regime is obtained from CEQUEAU simulations with the observed meteorological times series of the 1970-1999 period**.**

**Figure 2.** Mean inter-annual cycles of the interest hydroelectric production (HEPI) for the control period and two different future scenarios of annual temperature increase $\Delta T$.

**Figure 3. Storage requirement scheme** for the period 1970-1999 **(configuration HEP+RLM)**. Gray curves: day-to-day storage level trajectory required each year to reach the best possible resource / demand equilibrium, given the constraints; Black curve: mean inter-annual storage cycle.

**Figure 4. Variations of SWV, reservoir level, inflows and interest for hydroelectric production (HEPI)** from January 1977 to January 1981 for the meteorological control scenario (Ja: January, M: May, S: September).Top: Marginal value of storage water (SWV.m-3) for different reservoir storage levels corresponding to 10, 50 and 90 % of the capacity. Middle: Reservoir level (%) Bottom: Water inflow to the reservoir (blue curve, m3.s-1) and interest of hydroelectric production (red curve, V.kWh-1).

**Figure 5. SWV signature for the single hydroelectric production objective (HEP).** The mean inter-annual SWV variation obtained for the 1970-1999 period is plotted for three reservoir storage levels (10 %, 50 % and 90 % of storage capacity). For each storage level, the upper, middle, and lower curves correspond respectively to the 95th percentile, the mean and the 5th percentile of SWV calendar values obtained for the 30 years of the period.

**Figure 6. SWV signature for the reservoir level maintenance objective (RLM).** See Figure 4 for caption details. The 90 % curves are confounded with the x axis.

**Figure 7. SWV signature for the double-objective configuration (HEP+RLM).** See Figure 4 for caption details.

**Figure 8 : Sensitivity of storage requirement scheme to** temperature increase and/or precipitation decrease.

**Figure 9. Sensitivity of SWV signatures to temperature.** The different curves correspond to the control data set and to two scenarios of warming. The different columns correspond to storage levels of 10 % (left), 50 % (middle) and 90 % (right) of storage capacity. The objectives considered are the HEP (top graphs), the RLM (middle) and a combination of the two (bottom).

**Figure 10. Sensitivity of SWV to precipitation changes** in case of the double-objective configuration (HEP+RLM). The different columns correspond to storage levels of 10 % (left), 50 % (middle) and 90 % (right) of storage capacity.

**Figure 11: Sensitivity of SWV to changes of both precipitation and temperature** in case of the double-objective objective configuration (HEP+RLM). The different columns correspond to storage levels of 10 % (left), 50 % (middle) and 90 % (right) of storage capacity.

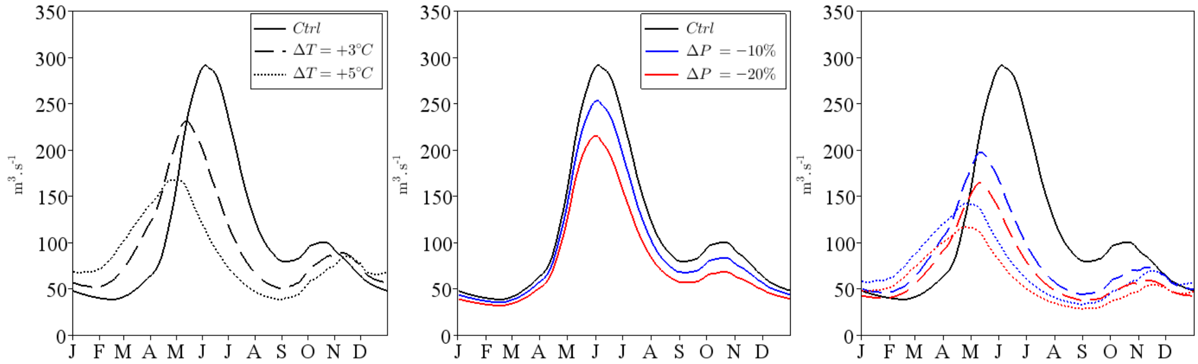


**Figure 1. Mean inter-annual cycles of daily inflow to the reservoir for control data** (black curve in all graphics, period 1970-1999) **and two future meteorological scenarios** (with prescribed changes of the mean annual temperature (ΔT) and precipitation (ΔP) over the period 2070-2099). Left: Changes in mean annual temperature only. Middle: Changes in mean annual precipitation only. Right: Changes in both annual precipitation and temperature. The control hydrological regime is obtained from CEQUEAU simulations with the observed meteorological times series of the 1970-1999 period.

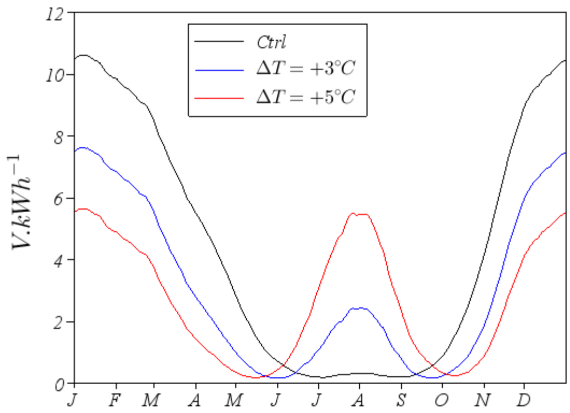


**Figure 2.** Mean inter-annual cycles of the interest hydroelectric production (HEPI) for the control period and two different future scenarios of annual temperature increase ΔT.

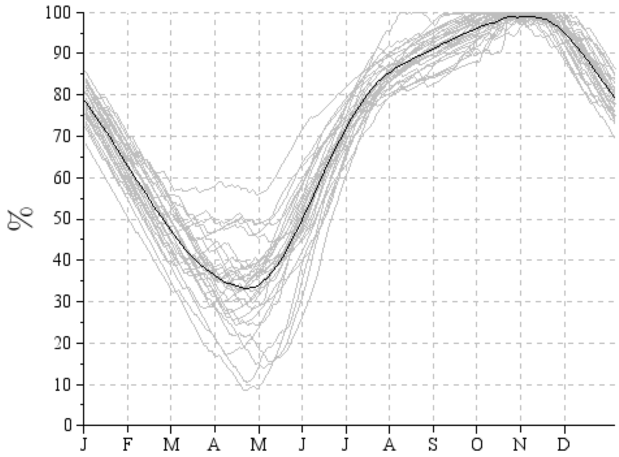


**Figure 3. Storage requirement scheme for the period 1970-1999 (configuration HEP+RLM).** Gray curves: day-to-day storage level trajectory required each year to reach the best possible resource / demand equilibrium, given the constraints; black curve: mean inter-annual storage cycle (storage signature).

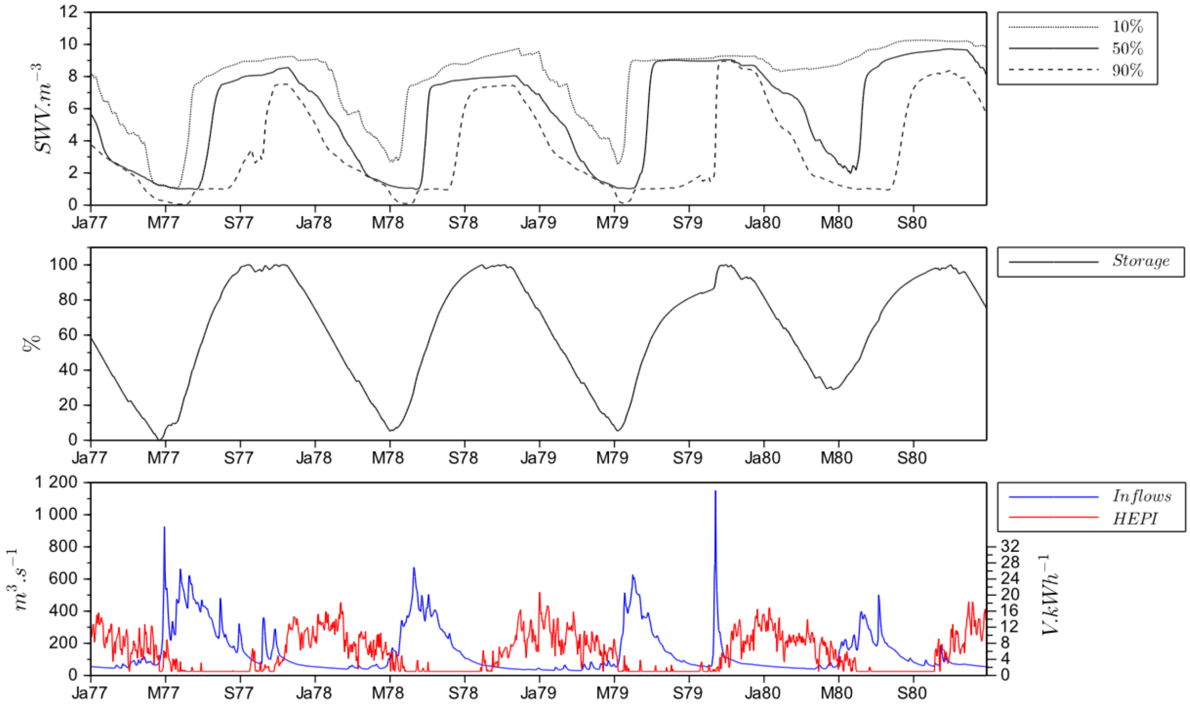


**Figure 4. Variations of SWV, reservoir level, inflows and interest for hydroelectric production (HEPI)** from January 1977 to January 1981 for the meteorological control scenario (Ja: January, M: May, S: September).Top: Marginal value of storage water (SWV.m$^{-3}$) for different reservoir storage levels corresponding to 10, 50 and 90 % of the capacity. Middle: Reservoir level (%). Bottom: Water inflow to the reservoir (blue curve, m$^{3}$.s$^{-1}$) and interest of hydroelectric production (red curve, V.kWh$^{-1}$).

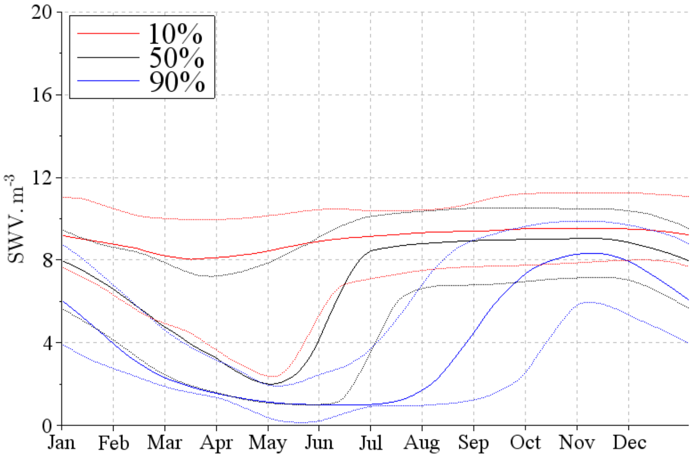


**Figure 5. SWV signature for the single hydroelectric production objective (HEP).** The mean inter-annual SWV variation obtained for the 1970-1999 period is plotted for three reservoir storage levels (10 %, 50 % and 90 % of storage capacity). For each storage level, the upper, middle, and lower curves correspond respectively to the 95$^{th}$ percentile, the mean and the 5$^{th}$ percentile of SWV calendar values obtained for the 30 years of the period.

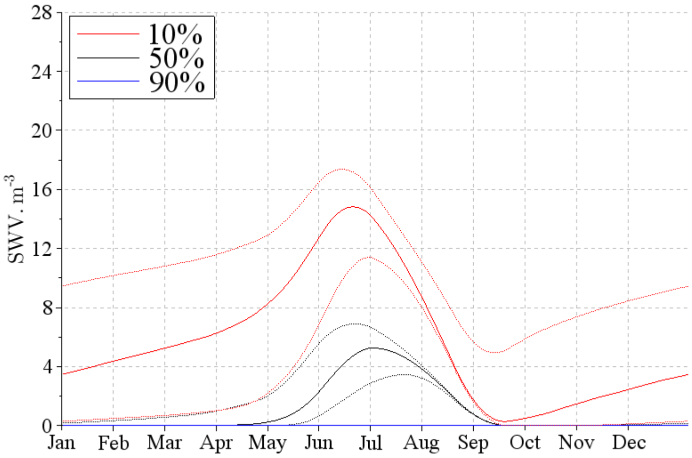


**Figure 6. SWV signature for the reservoir level maintenance objective (RLM).** See Figure 4 for caption details. The 90 % curves are confounded with the x axis.

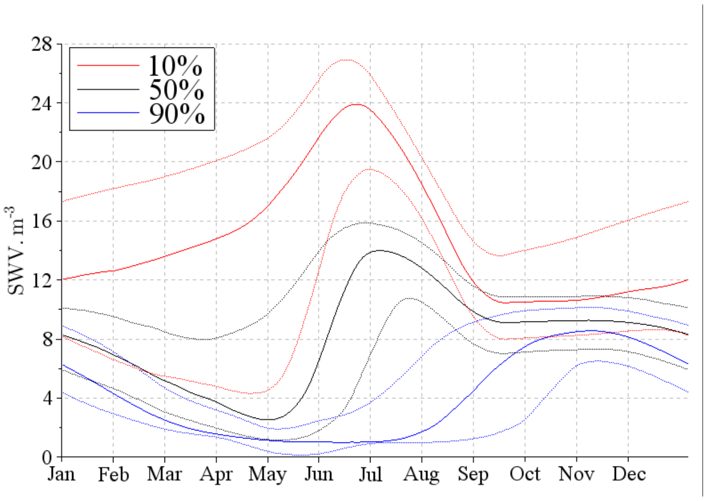


**Figure 7. SWV signature for the double-objective configuration (HEP+RLM).** See Figure 4 for caption details.

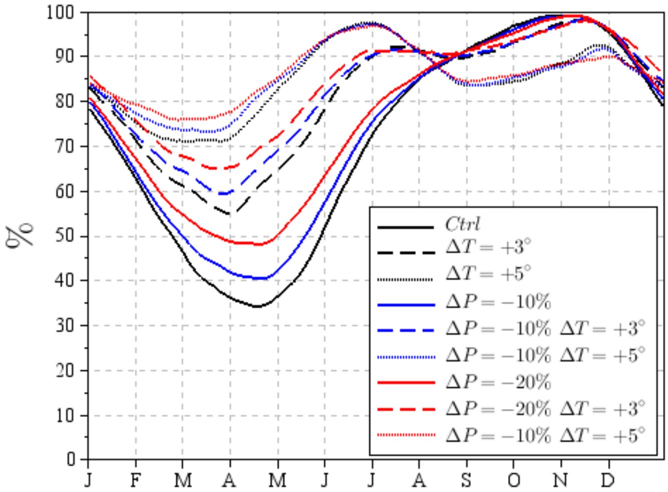


**Figure 8 : Sensitivity of storage signature to** temperature increase and/or precipitation decrease.

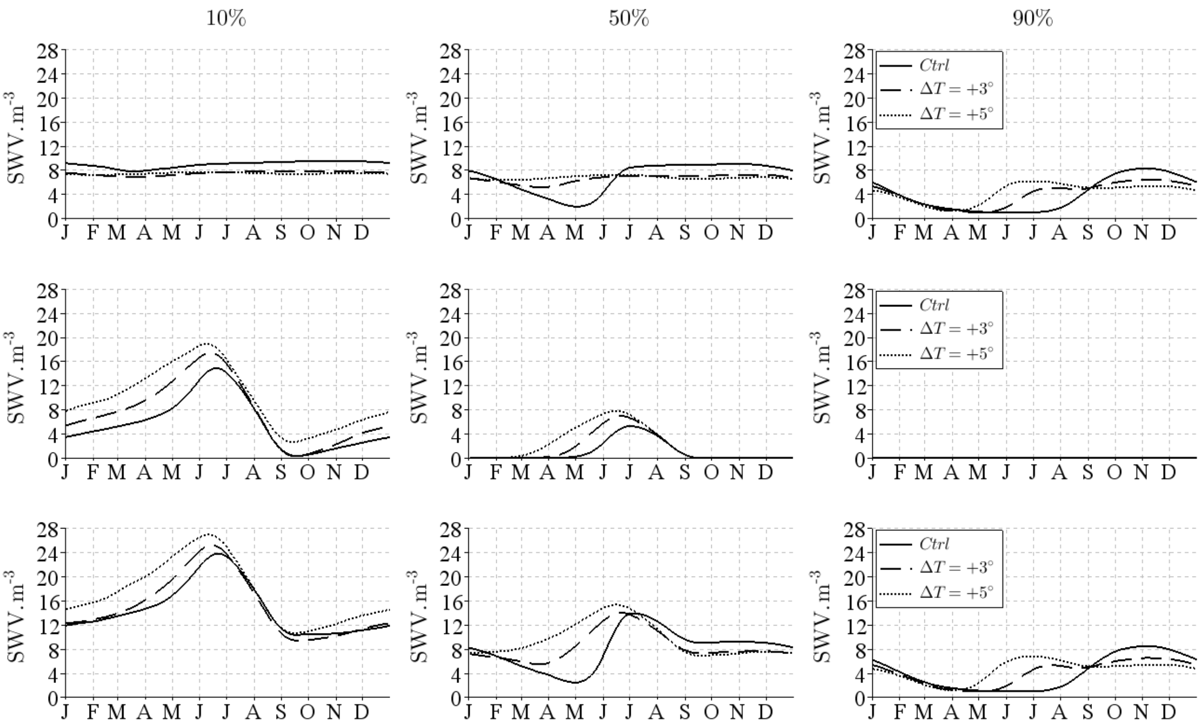


**Figure 9. Sensitivity of SWV signatures to temperature.** The different curves correspond to the control data set and to two scenarios of warming. The different columns correspond to storage levels of 10 % (left), 50 % (middle) and 90 % (right) of storage capacity. The objectives considered are the HEP (top graphs), the RLM (middle) and a combination of the two (bottom).

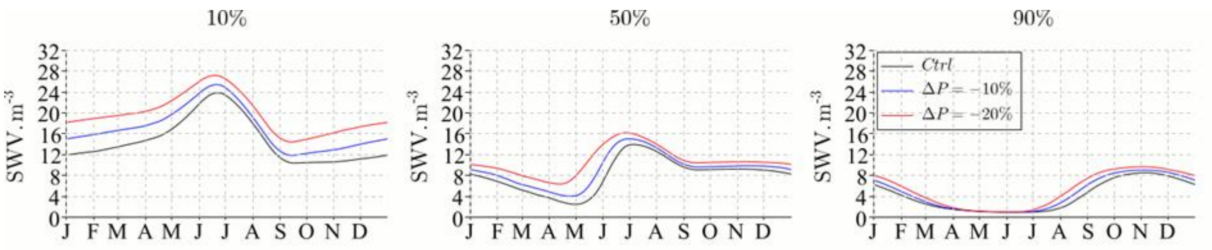


**Figure 10. Sensitivity of SWV signatures to precipitation changes** in case of the double-objective configuration (HEP+RLM). The different columns correspond to storage levels of 10 % (left), 50 % (middle) and 90 % (right) of storage capacity.

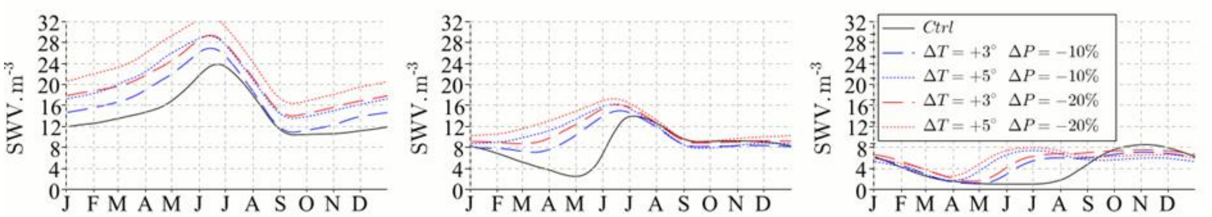


**Figure 11: Sensitivity of SWV signatures to changes of both precipitation and temperature** in case of the double-objective configuration (HEP+RLM). The different columns correspond to storage levels of 10 % (left), 50 % (middle) and 90 % (right) of storage capacity.